**Inter*net* Electronic Journal of Molecular Design**

August 2003, Volume 2, Number 8, Pages 511–526

Editor: Ovidiu Ivanciuc

Special issue dedicated to Professor Nenad Trinajstić on the occasion of the 65th birthday
Part 2

Guest Editors: Douglas J. Klein and Sonja Nikolić

# Three–Dimensional Molecular Field Analyses of Agonists for Tyramine Receptor which Inhibit Sex–Pheromone Production in *Plodia interpunctella*

Akinori Hirashima,[1] Tomohiko Eiraku,[2] Eiichi Kuwano,[1] and Morifusa Eto[3]

[1] Department of Applied Genetics and Pest Management, Faculty of Agriculture, Graduate School, Kyushu University, Fukuoka 812–8581, Japan
[2] Graduate School of Bioresource and Bioenvironmental Sciences, Kyushu University, Fukuoka 812–8581, Japan
[3] Professor Emeritus of Kyushu University,7–32–2 Aoba, Higashi–ku, Fukuoka 813–0025, Japan

Received: June 18, 2003; Revised: August 4, 2003; Accepted: August 6, 2003; Published: August 31, 2003

**Citation of the article:**
A. Hirashima, T. Eiraku, E. Kuwano, and M. Eto, Three–Dimensional Molecular Field Analyses of Agonists for Tyramine Receptor which Inhibit Sex–Pheromone Production in *Plodia interpunctella*, *Internet Electron. J. Mol. Des.* **2003**, *2*, 511–526, http://www.biochempress.com.

**Inter*net* Electronic Journal of Molecular Design**

**BioChem Press**
http://www.biochempress.com

# Three–Dimensional Molecular Field Analyses of Agonists for Tyramine Receptor which Inhibit Sex–Pheromone Production in *Plodia interpunctella*[#]

Akinori Hirashima,[1,*] Tomohiko Eiraku,[2] Eiichi Kuwano,[1] and Morifusa Eto[3]

[1] Department of Applied Genetics and Pest Management, Faculty of Agriculture, Graduate School, Kyushu University, Fukuoka 812–8581, Japan

[2] Graduate School of Bioresource and Bioenvironmental Sciences, Kyushu University, Fukuoka 812–8581, Japan

[3] Professor Emeritus of Kyushu University,7–32–2 Aoba, Higashi–ku, Fukuoka 813–0025, Japan

Received: June 18, 2003; Revised: August 4, 2003; Accepted: August 6, 2003; Published: August 31, 2003

*Internet Electron. J. Mol. Des*. **2003**, *2* (8), 511–526

**Abstract**

**Motivation.** In drug discovery, it is common to have measured activity data for a set of compounds acting upon a particular protein but not to have knowledge of the three–dimensional structure of the protein active site. In the absence of such three–dimensional information, one can attempt to build a hypothetical model of the receptor site that can provide insight about receptor–site characteristics. Such an analysis is known as a molecular–field analysis (MFA), which provides compact and quantitative descriptors which capture three–dimensional information about a putative receptor site.

**Method.** Several compounds were tested for inhibitory specificity using a modified radiochemical bioassay to monitor *de novo* pheromone production in *Plodia interpunctella*. All computational experiments were conducted with Cerius2 3.8 quantitative structure–activity relationship (QSAR) environment on a Silicon Graphics O2, running under the IRIX 6.5 operating system. Multiple conformations of each molecule were generated using the Boltzmann jump as a conformational search method.

**Results.** An MFA was generated from the 28 agonists for tyramine (TA) receptor which inhibited sex–pheromone production in *P. interpunctella*. 2–(Substituted benzylthio)–2–oxazoline (SBO) **2** had the highest potency, followed by SBO derivative **6** and **3**, substituted with 3–$CH_3$, 4–$CH_3$, and 3–$CF_3$, respectively, in inhibition of *de novo* pheromone production. The predictive character of the QSAR was further assessed using 4 agonists for TA receptor as test molecules.

**Conclusions.** The result may imply that the process of calculating an MFA treats the structures reasonably. The MFA could provide useful information in the characterization and differentiation of TA receptor. It may help to point the way towards developing extremely potent and relatively specific TA ligands, leading to potential insecticides, although further research on the comparison of the 3D QSAR is necessary.

**Keywords.** *Plodia interpunctella*; quantitative structure–activity relationship; molecular–field analysis; Cerius2; agonist for tyramine receptor.

[#] Dedicated to Professor Nenad Trinajstić on the occasion of the 65th birthday.

* Correspondence author; phone: +81–92–642–2856; fax: +81–92–642–2858; E–mail: ahirasim@agr.kyushu–u.ac.jp.

**Abbreviations and notations**

| | |
|---|---|
| AII, 2–(2,6–diethylphenylimino)imidazolidine | 3MDO, 2–(3–methylbenzylthio)–4,4'–dimethyl–2–oxazoline |
| AIO, 2–(arylimino)oxazolidine | 4MDO, 2–(4–methylbenzylthio)–4,4'–dimethyl–2–oxazoline |
| AIT, 2–(arylimino)thiazolidine | MFA, molecular–field analysis |
| BOA, 2–(3–methylbenzylthio)–2–oxazine | MMO, 2–(3–methylbenzylthio)–5–methyl–2–oxazoline |
| $Bsr^2$, bootstrap $r^2$ | OA, octopamine |
| cAMP, adenosine–3':5'–cyclic monophosphate | OAR3, octopamine receptor 3 |
| CAO, 2–(3–chlorobenzylamino)–2–oxazoline | PBAN, pheromone biosynthesis activating neuropeptide |
| CDM, chlordimeform | PLS, partial least squares |
| $CV–r^2$, cross–validated $r^2$ | PRESS, predicted sum of squares |
| GFA, genetic function approximation | QSAR, quantitative structure–activity relationship |
| G/PLS, genetic partial least squares | RSM, receptor–surface model |
| Hez, *Helicoverpa zea* | SBO, 2–(substitued benzylthio)–2–oxazoline |
| MBT, 2–(3–methylbenzylamino)–2–thiazolines | TA, tyramine |
| MCSG, maximum common subgroup | TMS, tetramethyl silane |

# 1 INTRODUCTION

Production of the pheromone blend is under the regulation of a neuropeptide termed pheromone biosynthesis activating neuropeptide (PBAN) [1–4]. The direct action of PBAN on the isolated pheromone gland tissue has been demonstrated by *in vitro* studies [5–10] showing stimulation of pheromone production in the presence of synthetic peptide. The exact tissue involved was delineated as the intersegmental membrane, which is situated between the 8th and 9th abdominal segments [11,12]. In *Helicoverpa armigera*, it has been shown that the pheromonotropic action due to PBAN in intact moths and decapitated moths, as well as pheromone gland incubations *in vitro*, is significantly inhibited by tyramine (TA) [11–13]. The inhibition was also reflected in a significant inhibitory effect on intracellular adenosine–3':5'–cyclic monophosphate (cAMP) levels, which were stimulated in the presence of PBAN. This inhibitory action is a result of a receptor (separate from the PBAN–receptor), which can be inhibited by pertussis toxin [12]. This provided evidence that the specific pheromonostatic–aminergic receptor is linked to a G–inhibitory protein. Female moths during specific periods call conspecific males when they emit their pheromone. The major pheromone component of Indian meal moth *Plodia interpunctella* was identified as (*Z*,*E*)–9,12–tetradecadienyl acetate [14–16] and the inhibitors of calling behavior and pheromone production have been reported in *P. interpunctella* [17], which inhibited PBAN–induced sex–pheromone production competitively with TA (unpublished data) and whose action was antagonized by yohimbine (unpublished data), an antagonist for the TA receptor [18].

TA showed stronger inhibitory activity of pheromone production than that of octopamine (OA) in *H. armigera*, and this action was nullified by yohimbine [11]. Some compounds, which inhibited sex–pheromone production and cAMP synthesis in *H. armigera*, have been found [19]. TA suppressed pheromone production in the silkworm moth, *Bombyx mori* and its target would be pheromone gland (unpublished data). In the studies with cloned receptors, evidence is emerging that the OA and TA receptors are couples to adenylate cyclase, positively and negatively respectively [20–26]. While it has been clearly shown that OA acts as a neuromediator in various insects, there

are few reports suggesting that TA might be a neuromediator in invertebrates [27]. Consequently, TA could not only be a biosynthetic precursor to OA, but may also play an independent role as a neuromediator, although it still remains to be clarified. Thus, the pheromonostatic receptor acting in a neuromodulatory role represents a novel type of TA receptor. It is therefore of critical importance to provide information on the pharmacological properties of this TA receptor types and subtypes.

Much attention has been directed recently at the octopaminergic system as a valid target in the development of safer and selective pesticides [28–30]. Structure–activity studies of various types of agonists and antagonists for the OA receptor were also reported using the nervous tissue of the migratory locust, *Locusta migratoria* L. [31–35]. However, information on the structural requirements of these agonists and antagonists for high OA–receptor ligands is still limited. It is therefore of critical importance to provide information on the pharmacological properties of this OA–receptor types and subtypes. Our interest in agonists for the OA receptor was aroused by the results of quantitative structure–activity relationship (QSAR) studies using various physicochemical parameters as descriptors [36–37] and receptor surface model (RSM) [38–39]. Furthermore, molecular modeling and conformational analysis were performed in Catalyst/Hypo to gain a better knowledge of the interactions between antagonists and the OA receptor 3 (OAR3) in order to understand the conformations required for binding activity [40]. A similar procedure was repeated using agonists for the OA receptor [41]. In drug discovery, it is common to have measured activity data for a set of compounds acting upon a particular protein but not to have knowledge of the three–dimensional structure of the protein active site. In the absence of such three–dimensional information, one can attempt to build a hypothetical model of the receptor site that can provide insight about receptor–site characteristics. Such an analysis is known as a molecular–field analysis (MFA), which provides compact and quantitative descriptors to capture three–dimensional information about a putative receptor site. Thus, the current work is aimed to perform 3D MFA on a set of agonists for TA receptor responsible for the inhibition of sex–pheromone production in *P. interpunctella*.

## 2 MATERIALS AND METHODS

### 2.1 Synthesis of Agonists for TA Receptor

The compounds reported here have been prepared according to the reported method [17]. 2–(Substituted benzylthio)–2–oxazolines (SBOs) **1**–**8**, **29**, 2–(3–methylbenzylthio)–2–oxazine (BOA) **9**, 2–(cinnamylthio)–2–oxazoline (CAO) **10**, 2–(3–methylbenzylthio)–4,4'–dimethyl–2–oxazoline (3MDO) **11**, 2–(4–methylbenzylthio)–4,4'–dimethyl–2–oxazoline (4MDO) **12**, and 2–(3–methylbenzylthio)–5–methyl–2–oxazoline (MMO) **13** were prepared from oxazolidine–2–thione and substituted benzylhalide in the presence of sodium hydride. 2–(Arylimino)oxazolidines (AIOs)

**14**–**20** were obtained by cyclodesulfurizing the corresponding thiourea with yellow mercuric oxide. AITs **21**–**23**, **30**–**31**, and 2–(3–methylbenzylamino)–2–thiazolines (MBT) **26** were synthesized by cyclization of the corresponding thiourea with conc. hydrochloric acid. 2–(2,6–Diethylphenylimino)imidazolidine (AII) **32** was prepared by refluxing the corresponding aniline and 1–acetyl–2–imidazolidone in phosphoryl chloride followed by hydrolysis. The structures of the compounds were confirmed by $^{1}$H–, $^{13}$C–NMR measured with a JEOL JNM–EX400 spectrometer at 400 MHz, tetramethyl silane (TMS) being used as an internal standard for $^{1}$H NMR, and elemental analytical data. Chlordimeform (CDM, 96% pure) **25** was a gift from Nihon Nohyaku Co. Ltd. (Osaka, Japan) and used after purification by column chromatography on silica gel.

## 2.2 Chemicals

DL–Adrenalin **24** hydrochloride was purchased from Tokyo Chem. Ind. Co. Ltd. (Tokyo, Japan); OA **27** and TA **28** were from Nacalai Tesque (Kyoto, Japan); Hez (*Helicoverpa zea*)–PBAN was from Peninsula Lab (Belmont, USA).

## 2.3 Biological Assay

### 2.3.1 Insect culture

The colony of *P. interpunctella* was raised on a diet of 80% ground rice, 10% glycerin, 5% brewer's yeast, and 5% honey at 28$^{o}$C and 70% RH in a 14:10 (light : dark) photoperiod as reported previously [17]. Larvae of wandering stage were pupated between pieces of paper carton and the resulting pupae were sexed, and males and females were emerged separately. Emerged virgin females were staged according to age.

### 2.3.2 *In vitro* pheromone–production bioassay

Compounds were tested for inhibitory specificity using a modified radiochemical bioassay to monitor *de novo* pheromone production [17]. Abdominal tips, containing the eighth and ninth abdominal segments with the attached intersegmental membrane, were removed from one day–old virgin females under sterile conditions during the first–third hour scotophase, using a dim red light for illumination. After preincubation in Pipes–buffered incubation medium [19] for 30 min, the intersegments were dried on tissue paper and then transferred individually to 10 μl medium containing 0.5 μCi [1–$^{14}$C]acetate in the presence or absence of 0.5 μM synthetic Hez–PBAN and test compounds. All incubations for pheromone production were performed at room temperature, maintaining the photoperiod. After the required incubation period (3 h) in order to measure the incorporation of [1–$^{14}$C]acetate into pheromone components, the glands were extracted in hexane, which was washed with water, and the amount of radioactivity of the hexane extract was measured using a liquid scintillation counter (LSC, Beckman LS 6500 multipurpose liquid scintillation analyzer) after adding scintillation cocktail (Clear–sol I). The concentration of the agonist at which

the pheromone production is inhibited by 50% (*K*i) was calculated by a sigmoidal curve–fitting program designed for log dose–probit activity analyses using a Macintosh personal computer system.

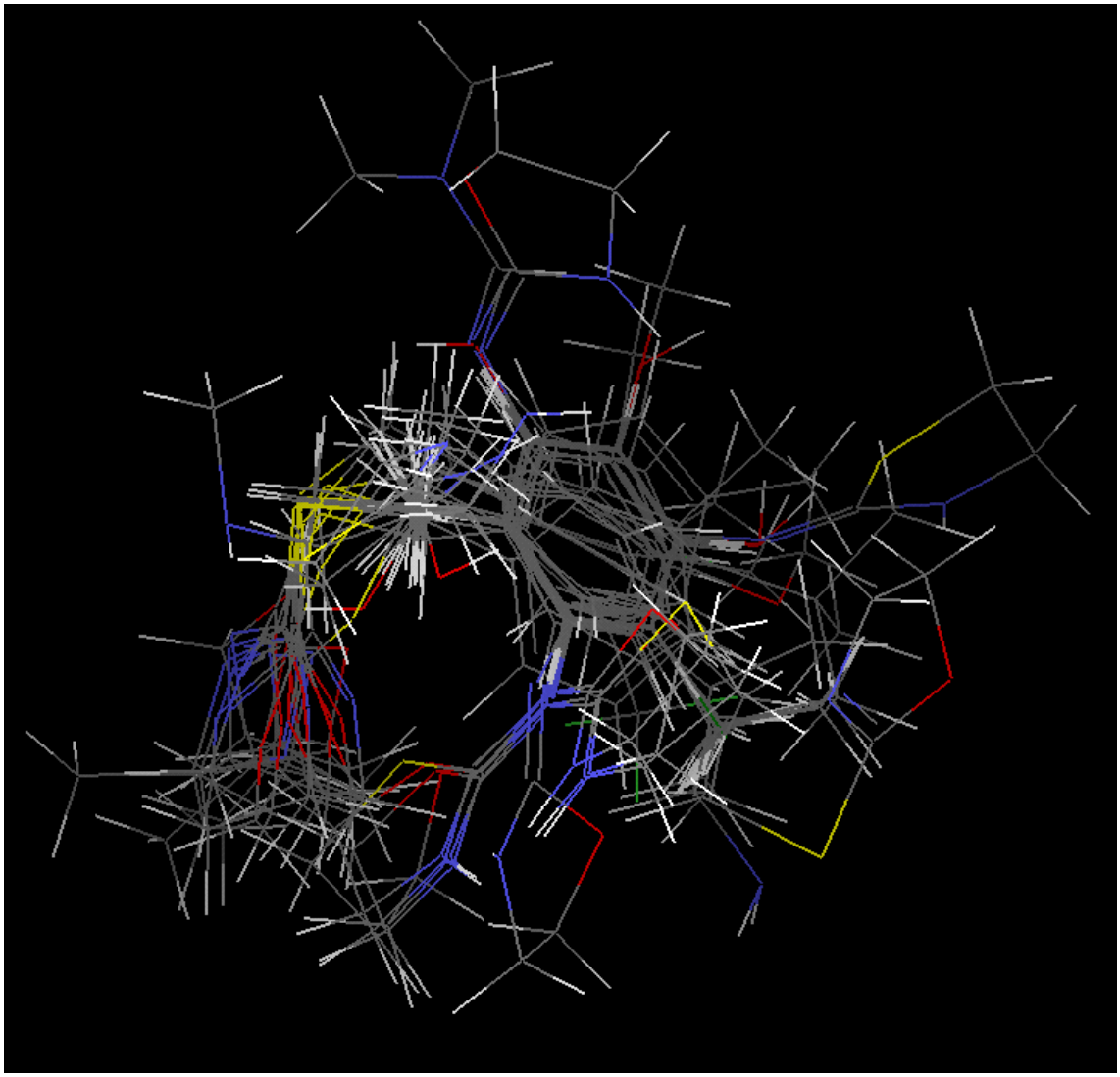

**Figure 1.** View of all the aligned study compounds **1**–**28**.

## 2.4 Computational Details

### 2.4.1 Molecular alignment

All computational experiments were conducted with Cerius2 3.8 QSAR environment from Accelrys (Burlington, MA) on a Silicon Graphics O2, running under the IRIX 6.5 operating system. Multiple conformations of each molecule were generated using the Boltzmann jump as a conformational search method. The upper limit of the number of conformations per molecule was 150. Each conformer was subjected to an energy minimization procedure to generate the lowest energy conformation for each structure. A conformer of the most active agonist **2** for the TA

receptor was selected as a standard reference to which all the structures in the study compounds were aligned through pair–wise superpositioning (Figure 1). The method used for performing the alignment was maximum common subgroup (MCSG) [42]. This method looks at molecules as points and lines, and uses the techniques of graph theory to identify patterns. It finds the largest subset of atoms in the shape reference compound that is shared by all the structures in the study table and uses this subset for alignment. A rigid fit of atom pairings was performed to superimpose each structure so that it overlays the shape reference compound. Naturally occurring S form was used for catecholamines adrenalin **24**, and R form was used for monophenolamines OA **27** in calculating the model.

### 2.4.2 MFA

MFA models are predictive and sufficiently reliable to guide the chemist in the design of novel compounds. These descriptors are used for predictive QSAR models. This approach is effective for the analysis of data sets where activity information is available but the structure of the receptor site is unknown. MFA attempts to postulate and represent the essential features of a receptor site from the aligned common features of the molecules that bind to it. This method generates multiple models that can be checked easily for validity. The MFA formalism calculates probe interaction energies on a rectangular grid around a bundle of active molecules. The surface is generated from a "Shape Field". The atomic coordinates of the contributing models are used to compute field values on each point of a 3D grid. Grid size was adjusted to default 2.00 Å, since decreasing grid size to 1.00 Å did not help to improve the model. MFA evaluates the energy between a probe (H+, $CH_3$, $CH_3$+, $CH_3$–, OH–, and Donor/Acceptor) and a molecular model at a series of points defined by a rectangular grid. Fields of molecules are represented using grids in MFA and each energy associated with an MFA grid point can serve as input for the calculation of a QSAR. These energies were added to the study table to form new columns headed according to the probe type. The charges of the target molecules and probes have not been calculated.

### 2.4.3 Genetic partial least squares (G/PLS)

Due to the large number of points used as independent variables, G/PLS [42] was used to derive the QSAR models. G/PLS, a variation of genetic function approximation (GFA), can be run as an alternative to the standard GFA algorithm. G/PLS is derived from the best features of two methods: GFA and partial least squares (PLS) and actually G/PLS gave better results than in cases GFA or PLS were used. Both GFA and PLS have been shown to be valuable analysis tools in cases where the data set has more descriptors than samples. In PLS, variables might be overlooked during interpretation or in designing the next experiment even though cumulatively they are very important. This phenomenon is known as “loading spread” [42]. In GFA, equation models have a randomly chosen proper subset of the independent variables. As a result of multiple linear

regression on each model, the best ones become the next generation and two of them produce an offspring. Models are collected that have a randomly chosen proper subset of the independent variables and then the collected models are evolved. A generation is the set of models resulting from performing multiple linear regression on each model; a selection of the best ones becomes the next generation. Cross–over operations are performed on these which take some variables from each of two models to produce an offspring. In addition, the best model from the previous generation is retained. This was repeated 10000 (default 5000) times. For other settings, all defaults were used. Loading spread does not occur because at most one of a set of colinear variables is retained in each model. Each generation has PLS applied to it instead of multiple linear regression, and so each model can have more terms in it without danger of over–fitting. G/PLS retains the ease of interpretation of GFA by back–transforming the PLS components to the original variables.

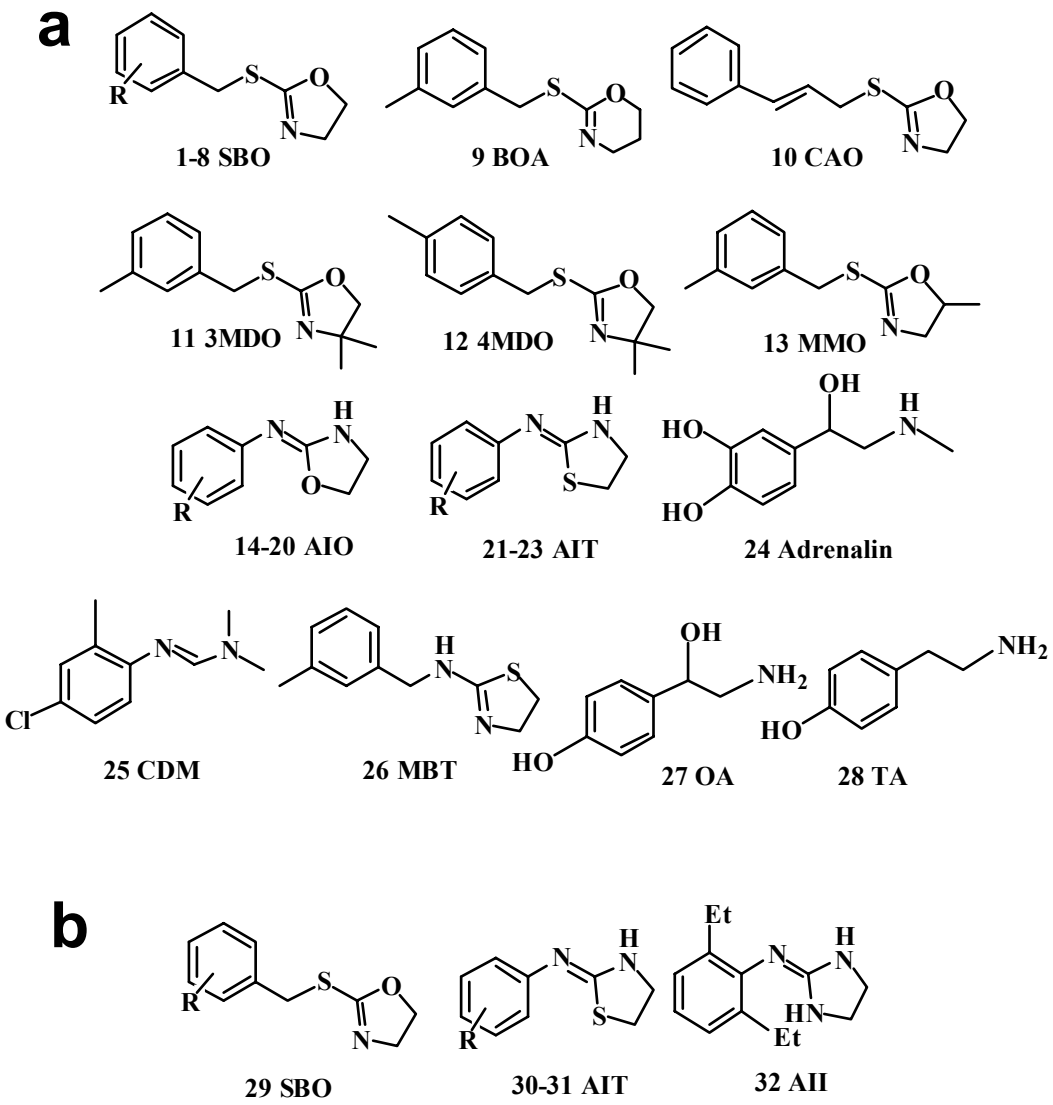


**Figure 2.** Structures of agonists for TA receptor used for regression analysis in study (a) and test (b) sets.

# 3 RESULTS AND DISCUSSION

A set of 28 molecules inhibited sex–pheromone production in *P. interpunctella*. The molecular structures and experimental biological activities are listed in Figure 2a and Table 1. 2–(Substituted benzylthio)–2–oxazoline (SBO) **2** had the highest potency, followed by SBO derivative **6** and **3**, substituted with 3–$CH_3$, 4–$CH_3$, and 3–$CF_3$, respectively, in inhibition of *de novo* pheromone production (Table 1). Activities of the agonists are expressed as their *K*i values in mM and activities range over two orders of magnitude (min. 0.088 mM and max. 6.46 mM). This set included a variety of types of molecules and for these types of training set; the use of the MFA generation tool was appropriate. This tool builds MFA for which the fit of individual molecules to an MFA can be correlated with the molecule's affinity.

**Table 1.** Regression Analysis of Structure–Activities for TA–Receptor Agonists in Study Set

| Compound | | *H+/* | | | | | | | | |
|---|---|---|---|---|---|---|---|---|---|---|
| No | R | *183* | *252* | *253* | *255* | *262* | *335* | *340* | *388* | *462* |
| | | | | | SBO | | | | | |
| **1** | 2–Me | –13.90 | 9.82 | 30.00 | 30.00 | 30.00 | 30.00 | 7.80 | 30.00 | 0.54 |
| **2** | 3–Me | –18.21 | 3.09 | 30.00 | 30.00 | –25.85 | 30.00 | 4.92 | 30.00 | 2.46 |
| **3** | 3–$CF_3$ | –5.69 | 30.00 | 30.00 | 30.00 | 30.00 | 30.00 | 6.29 | 30.00 | 12.03 |
| **4** | 3–MeO | –11.50 | –6.35 | 30.00 | 30.00 | 30.00 | 30.00 | –30.00 | 12.72 | 10.34 |
| **5** | 4–F | –6.93 | 13.10 | 30.00 | 30.00 | 30.00 | 30.00 | –12.38 | 14.76 | 11.19 |
| **6** | 4–Me | –19.13 | 7.52 | 30.00 | 30.00 | –19.89 | 30.00 | 11.47 | 30.00 | 6.52 |
| **7** | 4–MeO | –9.76 | –9.85 | 30.00 | –18.61 | –25.64 | 4.43 | 17.22 | 30.00 | –2.50 |
| **8** | 4–tBu | –9.13 | –0.91 | 30.00 | –22.43 | 30.00 | 30.00 | 3.45 | 30.00 | –0.30 |
| **9** | BOA | –21.51 | –4.13 | –14.45 | 30.00 | 30.00 | 30.00 | 30.00 | 30.00 | 0.27 |
| **10** | CAO | 2.62 | 0.08 | –0.12 | 4.64 | 3.33 | 7.85 | 9.12 | 30.00 | 4.95 |
| **11** | 3MDO | 30.00 | –5.16 | 30.00 | –20.35 | 30.00 | –3.01 | 30.00 | 30.00 | –1.66 |
| **12** | 4MDO | 30.00 | 0.31 | –10.70 | 30.00 | 30.00 | –28.38 | –2.26 | 6.56 | 0.47 |
| **13** | MMO | –13.99 | –2.21 | 30.00 | 30.00 | 30.00 | 30.00 | –7.62 | –3.88 | 4.53 |
| | | | | | AIO | | | | | |
| **14** | 2–Et | –1.49 | –1.69 | –3.32 | –1.32 | –7.00 | –12.92 | 3.79 | 5.27 | 30.00 |
| **15** | 2–iPr | –1.69 | –26.46 | 30.00 | –0.50 | –4.91 | 30.00 | 0.25 | –8.32 | 1.06 |
| **16** | 2–Me,6–Et | –0.98 | –2.88 | –6.72 | –0.58 | –2.69 | 2.76 | 2.56 | 30.00 | –5.79 |
| **17** | 2–Me,6–iPr | 0.06 | –4.43 | –7.35 | 2.19 | –2.50 | 30.00 | 1.57 | 30.00 | –21.59 |
| **18** | 2,6–$Et_2$ | 0.22 | –28.49 | 30.00 | –3.93 | –8.41 | 30.00 | 0.18 | 30.00 | 0.33 |
| **19** | 2–Et,6–iPr | 1.02 | –30.00 | 30.00 | 0.39 | –4.62 | 4.09 | –0.30 | 30.00 | –2.28 |
| **20** | 2,6–$iPr_2$ | 1.53 | 3.90 | –2.11 | 3.57 | 2.90 | 4.28 | 5.68 | 30.00 | 30.00 |
| | | | | | AIT | | | | | |
| **21** | 2,4,6–$Me_3$ | 0.92 | –3.17 | –4.33 | 2.57 | 0.19 | 4.11 | 30.00 | 30.00 | –3.66 |
| **22** | 2,6–$Me_2$ | –0.24 | –4.20 | –6.09 | 1.03 | –1.20 | 3.26 | 4.32 | 30.00 | –23.30 |
| **23** | 2,6–$Et_2$ | –3.53 | 30.00 | 30.00 | –2.93 | –9.20 | 6.31 | 1.45 | 30.00 | 30.00 |
| **24** | Adrenalin | –5.93 | –6.11 | 5.57 | 30.00 | 13.98 | 30.00 | –30.00 | 6.61 | 18.06 |
| **25** | CDM | 2.42 | –13.81 | –2.31 | 5.68 | –0.01 | 11.70 | 10.67 | 30.00 | 4.13 |
| **26** | MBT | –3.88 | –1.12 | –2.14 | –4.33 | 0.97 | 4.01 | 6.58 | 30.00 | 30.00 |
| **27** | OA | –4.16 | –7.20 | –16.47 | –5.79 | –5.56 | 8.18 | 7.35 | 12.83 | 30.00 |
| **28** | TA | 1.11 | 30.00 | 1.64 | 2.44 | –4.03 | 2.08 | 6.38 | 30.00 | 2.51 |

**Table 1.** (Continued)

| Compound | | | | p*K*i | | |
|---|---|---|---|---|---|---|
| No | R | *K*i (mM) | | Obs | Calc [a] | Dev [b] |
| | | SBO | | | | |
| **1** | 2–Me | 0.25 | (0.19–0.31) | 3.60 | 3.68 | –0.08 |
| **2** | 3–Me | 0.088 | (0.057–0.153) | 4.06 | 4.03 | 0.03 |
| **3** | 3–$CF_3$ | 0.124 | (0.082–0.183) | 3.91 | 3.95 | –0.04 |
| **4** | 3–MeO | 0.96 | (0.75–1.24) | 3.02 | 2.99 | 0.03 |
| **5** | 4–F | 0.56 | (0.44–0.70) | 3.25 | 3.29 | –0.04 |
| **6** | 4–Me | 0.096 | (0.070–0.129) | 4.02 | 3.93 | 0.09 |
| **7** | 4–MeO | 0.65 | (0.52–0.81) | 3.19 | 3.24 | –0.05 |
| **8** | 4–tBu | 2.34 | (1.25–5.24) | 2.63 | 2.46 | 0.17 |
| **9** | BOA | 0.93 | (0.74–1.21) | 3.03 | 3.12 | –0.09 |
| **10** | CAO | 1.82 | (1.09–3.38) | 2.74 | 2.70 | 0.04 |
| **11** | 3MDO | 0.25 | (0.19–0.34) | 3.60 | 3.62 | –0.02 |
| **12** | 4MDO | 0.29 | (0.22–0.38) | 3.54 | 3.54 | 0.00 |
| **13** | MMO | 0.68 | (0.55–0.82) | 3.17 | 3.14 | 0.03 |
| | | AIO | | | | |
| **14** | 2–Et | 4.67 | (3.92–5.56) | 2.33 | 2.23 | 0.10 |
| **15** | 2–iPr | 6.46 | (5.66–7.35) | 2.19 | 2.32 | –0.13 |
| **16** | 2–Me,6–Et | 3.07 | (2.14–4.67) | 2.51 | 2.65 | –0.14 |
| **17** | 2–Me,6–iPr | 5.83 | (5.40–6.26) | 2.23 | 2.25 | –0.02 |
| **18** | 2,6–$Et_2$ | 1.65 | (1.30–2.05) | 2.78 | 2.76 | 0.02 |
| **19** | 2–Et,6–iPr | 0.28 | (0.19–0.37) | 3.55 | 3.36 | 0.19 |
| **20** | 2,6–$iPr_2$ | 1.02 | (0.79–1.29) | 3.00 | 2.87 | 0.13 |
| | | AIT | | | | |
| **21** | 2,4,6–$Me_3$ | 3.03 | (2.48–3.65) | 2.52 | 2.48 | 0.04 |
| **22** | 2,6–$Me_2$ | 1.38 | (1.07–1.75) | 2.86 | 2.76 | 0.10 |
| **23** | 2,6–$Et_2$ | 0.27 | (0.18–0.40) | 3.57 | 3.70 | –0.13 |
| **24** | Adrenalin | 3.35 | (1.16–8.21) | 2.47 | 2.39 | 0.08 |
| **25** | CDM | 3.90 | (3.01–4.90) | 2.41 | 2.67 | –0.26 |
| **26** | MBT | 2.20 | (1.81–2.68) | 2.66 | 2.68 | –0.02 |
| **27** | OA | 5.11 | (2.23–10.47) | 2.29 | 2.42 | –0.13 |
| **28** | TA | 0.63 | (0.33–1.15) | 3.20 | 3.09 | 0.11 |

[a] Calculated with Eq. (1)
[b] When the predicted activity is overestimated, the deviation is obtained by calculating predicted activity subtracted by experimental value and indicated by minus. When the predicted activity is underestimated, the deviation is obtained by calculating experimental activity subtracted by predicted value.

Figure 3 shows **2** with the highest activity and **15** with the lowest activity embedded in an MFA generated from the agonist data set. A rigid fit was performed to superimpose each structure so that it overlays the shape reference compound **2**. The field of the entire agonist data set is represented and only the structures of **2** and **15** are embedded within the contours. The red surface represents a contour for those points that correspond to a proton probe to p*K*i of **2**. The ethyl chain of **15** is superimposed with the thiomethylene side chain of **3**. The red surface is embedded with the hetero ring of **15**, and **15** should be in a less desirable position for its activity, since **2** has higher activity than **15**.

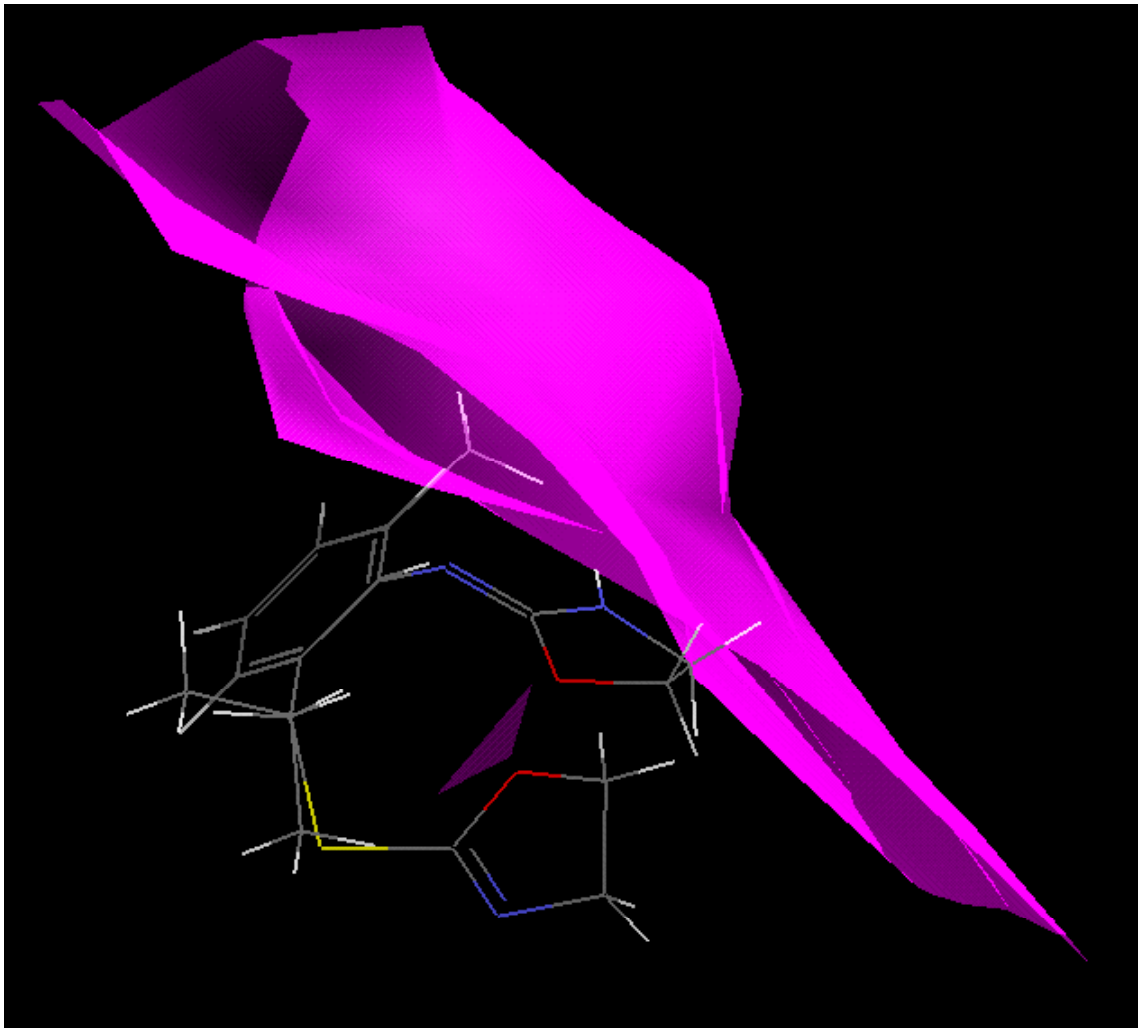

**Figure 3.** SBO **2** with the highest activity and **15** with the lowest activity embedded in an MFA generated from the agonist data set for the TA receptor. The field of the entire agonist data set is represented and only the structures of **2** and **15** are embedded within the contours. The red surface represents a contour for those points that correspond to a proton probe to p*K*i of **2**. The ethyl chain of **15** is superimposed with the thiomethylene side chain of **2**.

In order to quantitatively understand the relationship between the biological activities of agonists for TA receptor with MFA parameters, regression analysis was applied to represent 28 study compounds listed in Figure 2a and Table 1, leading to Eq. (1). The number of variables for Eq. (1) was 576 and ten percent of the variables were automatically used as independent X variables in the generation of QSAR. In Eq. (1), the descriptors *H+/a*, *H+/b*, and *H+/c*, etc are the energies between a proton probe and the molecule at the rectangular points a, b, and c, etc respectively:

$$\begin{aligned} \text{p}Ki = {} & 1.94512 + 0.000743(H+/183 + 4.15491)^2 + 0.000293(H+/252 - 7.20198)^2 + \\ & 0.000622(H+/253)^2 + 0.0004(H+/255 + 22.43)^2 + 0.000444(H+/262 - 0.97122)^2 - \\ & 0.000597(H+/335)^2 - 0.000237(H+/340)^2 + 0.000519(H+/388)^2 + 0.000168(H+/462 - \\ & 0.536533)^2 \end{aligned} \quad (1)$$

where $n$ = 28, $r^2$ = 0.965, $CV\text{–}r^2$ = 0.903, PRESS = 0.823, and $Bsr^2$ = 0.964±0.001. The term $n$

means the number of data points; *r*–squared ($r^2$), the square of the correlation coefficient, which is used to describe the goodness of fit of the data of the study compounds to the QSAR model; cross–validated $r^2$ ($CV–r^2$), a squared correlation coefficient generated during a validation procedure using the equation: $CV–r^2$ = (SD – PRESS)/SD; predicted sum of squares (PRESS), the sum of overall compounds of the squared differences between the actual and the predicted values for the dependent variables; SD, the sum of squared deviations of the dependent variable values from their mean. The PRESS value is computed during a validation procedure for the entire training set. The larger the PRESS value, the more reliable is the equation.

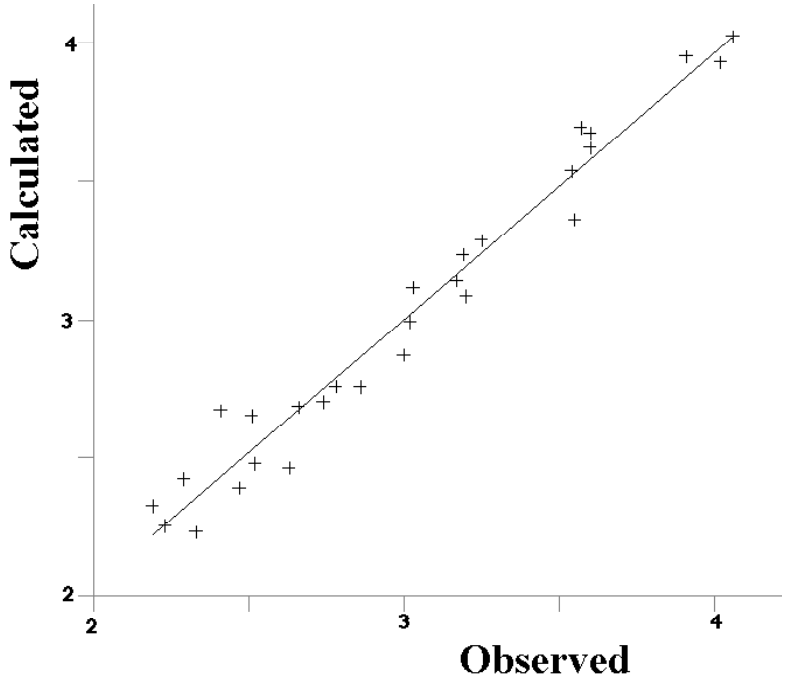


**Figure 4.** Correlation of observed p*K*i values (horizontal) versus calculated p*K*i values (vertical) from Table 1 using Eq. (1).

A $CV–r^2$ is usually smaller than the overall $r^2$ for a QSAR equation. It is used as a diagnostic tool to evaluate the predictive power of an equation generated using the G/PLS method. Cross–validation is often used to determine how large a model (number of terms) can be used for a given data set. For instance, the number of components retained in GFA can be selected to be that which gives the highest $CV–r^2$. Leave–3–out cross validation was run. The validation procedure uses the data set from which the model is derived and check the data for internal consistency. The procedure derives a new model using a reduced set of observations. Each time a new equation is generated, one row is excluded from the calculation. Each new equation is used to predict the activity of the molecule that was not included in the new–model set. This is repeated until all compounds have been deleted and predicted only once. Bootstrap $r^2$ ($Bsr^2$) is the average squared correlation coefficient calculated during the validation procedure [42]. A $Bsr^2$ is computed from the subset of variables used one–at–a–time for the validation procedure. It can be used more than one time in

computing the $r^2$ statistic. Table 1 depicts structures of agonists for TA receptor, their experimental *K*i values, calculated p*K*i values using Eq. (1), and difference between observed and calculated p*K*i values. Correlations (observed versus calculated from Table 1) are plotted in Figure 4. When the predicted activity is overestimated, the deviation is obtained by calculating predicted activity subtracted by experimental value and indicated by minus. When the predicted activity is underestimated, the deviation is obtained by calculating experimental activity subtracted by predicted value. The agonists for TA receptor inhibited calling behavior [43] and PBAN–induced sex–pheromone production [44] in *P*. *interpunctella*. TA also suppressed pheromone production in *B*. *mori* (unpublished data). Thus, TA plays an independent role as a neuromediator in regulating pheromone production. The MFA in this study was statistically significant and used to correctly predict the activities of a set of training molecules, indicating that these models could be useful tools to design active agonists for TA receptor.

**Table 2.** Regression Analysis of Structure–Activities for TA–Receptor Agonists in Test Set

| Compound | | *H+/* | | | | | | | | |
|---|---|---|---|---|---|---|---|---|---|---|
| No | R | *183* | *252* | *253* | *255* | *262* | *335* | *340* | *388* | *462* |
| | | | | | SBO | | | | | |
| **29** | H | 30.00 | –4.26 | 30.00 | –19.56 | 30.00 | –1.69 | 0.46 | –11.10 | 4.99 |
| | | | | | AIT | | | | | |
| **30** | 2,4–$Me_2$ | 0.85 | –3.52 | –4.67 | 2.58 | 0.19 | 4.50 | –1.06 | 30.00 | –3.60 |
| **31** | 2–Et,6–iPr | –1.25 | –29.72 | 30.00 | 0.32 | –6.46 | 30.00 | 0.68 | 30.00 | 2.09 |
| **32** | AII | –1.65 | 30.00 | –12.12 | 0.24 | –2.17 | 3.94 | 2.16 | 30.00 | 30.00 |

**Table 2.** (Continued)

| Compound | | | | p*K*i | | |
|---|---|---|---|---|---|---|
| No | R | | *K*i (mM) | Obs | Calc [a] | Dev [b] |
| | | | SBO | | | |
| **29** | H | 1.97 | (1.15–4.61) | 2.71 | 3.44 | –0.73 |
| | | | AIT | | | |
| **30** | 2,4–$Me_2$ | 2.12 | (1.82–2.48) | 2.67 | 2.69 | –0.02 |
| **31** | 2–Et,6–iPr | 0.82 | (0.56–1.15) | 3.09 | 2.82 | 0.27 |
| **32** | AII | 4.05 | (2.66–6.76) | 2.39 | 3.26 | –0.87 |

[a, b] See footnote to Table 1

Once the desired MFA has been constructed, all the structures in the test sets were evaluated against the model. The evaluation consists of computing several energetic descriptors that are based upon the interactions between ligand and model. By using receptor data to develop a QSAR model, the goodness of fit can be evaluated between a candidate structure and a postulated pseudo–receptor. The predictive character of the QSAR was further assessed using 4 agonists for TA receptor as test molecules, whose structures are shown in Figure 2b, outside of the training set. The best statistically significant Eq. (1) was applied to access these agonists. The predicted values of these molecules are listed in Table 2, which depicts agonists, their experimental *K*i values, calculated p*K*i values using Eq. (1), and difference between observed and calculated p*K*i values.

The process of evaluating the MFA for agonists for TA receptor treat these agonists reasonably and the activities of agonists **29–32** were reasonably predicted.

## 4 CONCLUSIONS

MFAs are quantitative and differ from pharmacophore models [43], which are qualitative, in that the former tries to capture essential information about the receptor, while the latter only captures information about the similarity of the compounds that bind. MFA attempts to postulate and represent the essential features of a receptor site itself, rather than the common features of the molecules that bind to it. MFAs tend to be geometrically overconstrained (and topologically neutral) since, in the absence of steric variation in a region, they assume the tightest steric surface which fits all training compounds. MFAs do not contain atoms, but try to directly represent the essential features of an active site by assuming complementarity between the shape and properties of the receptor site and the set of binding compounds. The MFA application uses 3D surfaces that define the shape of the receptor site. The global minimum of the most active compound **2** in the study compounds (based on the value in the activity column) was made as the active conformer. When there is no information on the actual "active conformation" of the ligands, MFA does not really describe the receptor; it describes a self–consistent field around the molecules that can explain activity. It really is just one of possibly many self–consistent models that fit the biological activity data. This model ought to be predictive and sufficiently reliable to guide the chemist in the design of novel compounds. These descriptors were used for predictive QSAR models. This approach is effective for the analysis of data sets where activity information is available but the structure of the receptor site is unknown.

TA is not likely to penetrate either the cuticle or the central nervous system of insects effectively, since it is fully ionized at physiological pH. Derivatization of the polar groups would be one possible solution to this problem in trying to develop potential pest–control agents. The above MFA studies show that phenyl ring substitution requirements for agonists differ substantially from each other and other various types of agonists for TA receptor could be potent, although the type of compounds tested here is still limited to draw any conclusions. The MFA could provide useful information in the characterization and differentiation of the TA receptor. The agonists for TA receptor showed reasonable predicted activities according to Eq. (1). The result may imply that the process of calculating an MFA treats these structures reasonably. It may help to point the way towards developing extremely potent and relatively specific TA ligands, leading to potential insecticides, although further research on the comparison of the 3D QSAR is necessary. In order to optimize the activities of these compounds as TA ligands, more detailed experiments are in progress.

## Acknowledgment

This work was supported in part by a Grant–in–Aid for Scientific Research from the Ministry of Education, Science, and Culture of Japan.

# 5 REFERENCES

[1] A. K. Raina, Neuroendocrine control of sex pheromone biosynthesis in Lepidoptera, *Ann*. *Rev*. *Entomol*. **1993**, *38*, 329–349.
[2] P. W. K. Ma and W. Roelofs, Calcium involvement in the stimulation of sex pheromone production by PBAN in the European Corn Borer, *Ostrinia nubilalis* (Lepidoptera: Pyralidae), *Insect Biochem*. *Molec*. *Biol*. **1995**, *25*, 467–473.
[3] A. Rafaeli and C. Gileadi, Neuroendocrine control of pheromone production in moths, *Invert*. *Neurosci*. **1997**, *3*, 223–229.
[4] R. A. Jurenka, Signal transduction in the stimulation of sex pheromone biosynthesis in moths, *Arch*. *Insect Biochem*. *Physiol*. **1996**, *33*, 245–258.
[5] V. Soroker and A. Rafaeli, *In vitro* hormonal stimulation of acetate incorporation by *Heliothis armigera* pheromone glands, *Insect Biochem*. **1989**, *19*, 1–9.
[6] A. Rafaeli, V. Soroker, B. Kamensky, and A. K. Raina, Action of PBAN on *in vitro* pheromone glands of *Heliothis armigera* females, *J*. *Insect Physiol*. **1990**, *36*, 641–646.
[7] R. Arima, K. Takahara, T. Kadoshima, F. Numazaki, T. Ando, M. Uchiyama, H. Nagasawa, A. Kitamura, and A. Suzuki, Hormonal regulation of pheromone biosynthesis in the silkworm moth *Bombyx mori* (Lepidoptera: Bombycidae), *Appl*. *Entomol*. *Zool*. **1991**, *26*, 137–148.
[8] R. A. Jurenka, E. Jacquin, and W. L. Roelofs, Stimulation of pheromone biosynthesis in the moth *Helicoverpa zea*, Action of a brain hormone on pheromone glands involves $Ca^{2+}$ and cAMP as second messengers, *Proc*. *Natl*. *Acad*. *Sci*. *USA* **1991**, *88*, 8621–8625.
[9] A. Fonagy, S. Matsumoto, L. Schoofs, A. De Loof, and T. Mitsui, *In vivo* and *in vitro* pheromonotropic activity of two locustatachykinin peptides in *Bombyx mori*, *Biosci*. *Biotech*. *Biochem*. **1992**, *56*, 1692–1693.
[10] S. Matsumoto, R. Ozawa, T. Nagamine, G.–H. Kim, K. Uchiumi, T. Shono, and T. Mitsui, Intracellular transduction in the regulation of pheromone biosynthesis of the silkworm, *Bombyx mori:* Suggested involvement of calmodulin and phosphoprotein phosphatase, *Biosci*. *Biotech*. *Biochem*. **1995**, *59*, 560–562.
[11] A. Rafaeli and C. Gileadi, Modulation of the PBAN–induced pheromonotropic activity in *Helicoverpa armigera*, *Insect Biochem*. *Molec*. *Biol*. **1995**, *25*, 827–834.
[12] A. Rafaeli and C. Gileadi, Down regulation of pheromone biosynthesis: Cellular mechanisms of pheromonostatic responses, *Insect Biochem*. *Molec*. *Biol*. **1996**, *26*, 797–807.
[13] A. Rafaeli, C. Gileadi, Y. Fan, and C. Meixun, Physiological mechanisms of pheromonostatic responses: effects of adrenergic agonists and antagonists on moth pheromone biosynthesis, *J*. *Insect Physiol*. **1997**, *43*, 261–269.
[14] Y. Kuwahara, C. Kitamura, S. Takahashi, H. Hara, S. Ishii, and H. Fukami, Sex pheromone of the almond moth and Indian meal moth: cis–9, trans–12–tetradecadienyl acetate, *Science* **1971**, *171*, 801–802.
[15] U. E. Brady, J. H. Tumlinson, R. G. Brownlee, and R. M. Silverstein, Sex stimulant and attractant in the Indian meal moth and in the almond moth, *Science* **1971**, *171*, 802–804.
[16] J. Zhu, C. Ryne, C. R. Unelinus, P. G. Valeur, and C. Lofstedt, Reidentification of the female sex pheromone of the Indian meal moth *Plodia interpunctella*: evidence for a four–component pheromone blend, *Entomol*. *Exp*. *Appl*. **1999**, *92*, 137–146.
[17] A. Hirashima, T. Eiraku, Y. Watanabe, E. Kuwano, E. Taniguchi, and M. Eto, Identification of novel inhibitors of calling and *in vitro* [$^{14}$C]acetate incorporation by pheromone glands of *Plodia interpunctella*, *Pest Manag*. *Sci*. **2001**, *57*, 713–720.
[18] L. Hiripi, S. Juhos, and R. G. Downer, Characterization of tyramine and octopamine receptors in the insect (Locusta migratoria migratorioides) brain, *Brain Res*. **1994**, *633*, 119–126.
[19] A. Rafaeli, C. Gileadi, and A. Hirashima, Identification of novel synthetic octopamine receptor agonists which inhibit moth sex pheromone production, *Pestic*. *Biochem Physiol* **1999**, *65*, 194–204.
[20] S. Arakawa, J. D. Gocayne, W. R. McCombie, D. A. Urquhart, L. M. Hall, C. M. Fraser, and J. C. Venter, Cloning, localization, and permanent expression of a *Drosophila* octopamine receptor, *Neuron* **1990**, *4*, 343–354.
[21] W. Blenau, S. Balfanz, and A. Baumann, Amtyr1: characterization of a gene from honeybee (*Apis mellifera*) brain encoding a functional tyramine receptor, *J*. *Neurochem*. **2000**, *74*, 900–908.
[22] D.–J. Chang, X.–C. Li, Y.–S. Lee, H.–K. Kim, U. S. Kim, N. J. Cho, X. Lo, K. R. Weiss, E. R. Kandel, and B.–K. Kaang, Activation of a heterologously expressed octopamine receptor coupled only to adenylyl cyclase produces

all the features of presynaptic facilitation in aplysia sensory neurons, *Proc. Natl. Acad. Sci. USA*. **2000**, *97*, 1829–1834.
[23] C. C. Gerhardt, R. A. Bakker, G. J. Piek, R. J. Planta, E. Vreugdenhil, J. E. Leysen, and H. Van Heerikhuizen, Molecular cloning and pharmacological characterization of a molluscan octopamine receptor, *Mol. Pharmac.* **1997**, *51*, 293–300.
[24] K.–A. Han, N. S. Millar, and R. L. Davis, A novel octopamine receptor with preferential expression in *Drosophila* mushroom bodies, *J. Neurosci*. **1998**, *18*, 3650–3658.
[25] F. Saudou, N. Amlaiky, J.–L. Plassat, E. Borrelli, and R. Hen, Cloning and characterization of a *Drosophila* tyramine receptor, *EMBO J*. **1990**, *9*, 3611–3617.
[26] J. Vanden Broeck, V. Vulsteke, R. Huybrechts, and A. De Loof, Characterization of a cloned locust tyramine receptor cDNA by functional expression in permanently transformed *Drosophila* S2 cells, *J. Neurochem*. **1995**, *64*, 2387–2395.
[27] H. A. Robertson and A. V. Juorio, Octopamine and some related noncatecholic amines in invertebrate nervous systems, *Internat. Rev. Neurobiol*. **1976**, *19*, 173–224.
[28] K. R. Jennings, D. G. Kuhn, C. F. Kukel, S. H. Trotto, and W. K. Whiteney, A biorationally synthesized octopaminergic insecticide: 2–(4–chloro–*o*–toluidino)–2–oxazoline, *Pestic. Biochem. Physiol*. **1988**, *30*, 190–197.
[29] A. Hirashima, Y. Yoshii, and M. Eto, Action of 2–aryliminothiazolidines on octopamine–sensitive adenylate cyclase in the American cockroach nerve cord and on the two–spotted spider mite *Tetranycus urticae* Koch, *Pestic. Biochem. Physiol*. **1992**, *44*, 101–107.
[30] S. M. M. Ismail, R. A. Baines, R. G. H. Downer, and M. A. Dekeyser, Dihydrooxadiazines: Octopaminergic system as a potential site of insecticidal action, *Pestic. Sci*. **1996**, *46*, 163–170.
[31] T. Roeder and J. A. Nathanson, Characterization of insect neuronal octopamine receptors (OA3 receptors), *Neurochem. Res*. **1993**, *18*, 921–925.
[32] T. Roeder and M. Gewecke, Octopamine receptors in locust nervous tissue, *Biochem. Pharm*. **1990**, *39*, 1793–1797.
[33] T. Roeder, A new octopamine receptor class in locust nervous tissue, the octopamine 3 (OA3) receptor, *Life Science* **1992**, *50*, 21–28.
[34] T. Roeder, Pharmacology of the octopamine receptor from locust central nervous tissue (OAR3), *Br. J. Pharmac.* **1995**, *114*, 210–216.
[35] T. Roeder, High–affinity antagonists of the locust neuronal octopamine receptor, *Eur. J. Pharmac.* **1990**, *191*, 221–224.
[36] A. Hirashima, K. Shinkai, C. Pan, E. Kuwano, E. Taniguchi, and M. Eto, Quantitative structure–activity studies of octopaminergic ligands against *Locust migratoria* and *Periplaneta americana*, *Pestic. Sci*. **1999**, *55*, 119–128.
[37] C. Pan, A. Hirashima, J. Tomita, E. Kuwano, E. Taniguchi, and M. Eto, Quantitative structure–activity relationship studies and molecular modelling of octopaminergic 2–(substituted benzylamino)–2–thiazolines and oxazolines against nervous system of *Periplaneta americana* L., *Internet J. Sci.–Biol. Chem*. **1997**, *1*, http://www.netsci–journal.com/97v1/97013/index.htm.
[38] A. Hirashima, C. Pan, J. Tomita, E. Kuwano, E. Taniguchi, and M. Eto, Quantitative structure–activity studies of octopaminergic agonists and antagonists against nervous system of *Locusta migratoria*, *Bioorg. Med. Chem*. **1998**, *6*, 903–910.
[39] A. Hirashima, E. Kuwano, and M. Eto, Three dimensional receptor surface model of octopaminergic agonists for the locust neuronal octopamine receptor, *Internet Electron. J. Mol. Des.* **2003**, *2*, 274–287, http://www.biochempress.com.
[40] C. Pan, A. Hirashima, E. Kuwano, and M. Eto, Three–dimensional pharmacophore hypotheses for the locust neuronal octopamine receptor (OAR3): 1. Antagonists, *J. Mol. Model*. **1997**, *3*, 455–463.
[41] A. Hirashima, C. Pan, E. Kuwano, E. Taniguchi, and M. Eto, Three–dimensional pharmacophore hypotheses for the locust neuronal octopamine receptor (OAR3): 2. Agonists, *Bioorg. Med. Chem*. **1999**, *7*, 1437–1443.
[42] Cerius2 tutorial, Accelrys Inc., http://www.accelrys.com/cerius2.
[43] A. Hirashima, T. Eiraku, E. Kuwano, E. Taniguchi, and M. Eto, Three–dimensional pharmacophore hypotheses of octopamine receptor responsible for the inhibition of sex–pheromone production in *Plodia interpunctella*, *Internet Electron. J. Mol. Des*. **2002**, *1*, 37–51, http://www.biochempress.com.
[44] A. Hirashima, Y. Shigeta, T. Eiraku, and E. Kuwano, Inhibitors of calling behavior of *Plodia interpunctella*, *J. Insect Sci*. **2003**, *3*, 4, http://insectscience.org/3.4/.

## Biographies

**Akinori Hirashima**, Ph.D., is associate professor of pesticidal chemistry at Kyushu University at Fukuoka, Japan. Dr. Hirashima formulated the investigation into the structural design of agonists for octopamine/tyramine receptor. After obtaining a Ph.D. degree in synthesis and stereochemistry of organophosphorus insecticides from the Kyushu

University in Fukuoka, Dr. Hirashima undertook postdoctoral research with Professor John E. Casida at the Environmental Chemistry and Toxicology Laboratory at the University of California at Berkeley, USA. More recently, Dr. Hirashima has collaborated on projects with Professor Hans–J. Riebel of Chemistry Department at the Bayer AG., Germany and Dr. A. Rafaeli of Pheromone Lab. at Volcani Centre, Israel.

**Tomohiko Eiraku**, M.Sci., was graduate student of pesticidal chemistry at Kyushu University at Fukuoka, Japan. Mr. Eiraku formulated the investigation on inhibitors of calling behaviour and *in vitro* pheromone biosynthesis into the structural design.

**Eiichi Kuwano**, Ph.D., is professor of pesticidal chemistry at Kyushu University at Fukuoka, Japan. Dr. Kuwano formulated the investigation into the structural design of juvenile–hormone agonists. After obtaining a Ph.D. degree in synthesis of s–triazine derivatives from amino acids and peptides and their biological activities from the Kyushu University in Fukuoka, Dr. Kuwano undertook postdoctoral research with Professor T. Roy Fukuto at the Department of Entomology at the University of California at Riverside. More recently, Dr. Kuwano has collaborated on projects with Professor Bruce D. Hammock of the Department of Entomology at the University of California at Davis.

**Morifusa Eto**, Ph.D., is professor emeritus of pesticidal chemistry at Kyushu University at Fukuoka, Japan. Dr. Eto investigated into the structural design of organophosphorus insecticides. After obtaining a Ph.D. degree in cyclic phosphorus esters with toxicity from the Kyushu University in Fukuoka, Dr. Eto undertook postdoctoral research with Professor John E. Casida at the Department of Entomology at the University of Wisconsin at Madison.